Electronic Supplementary Material (ESI) for Journal of Materials Chemistry A.

Nanopore Confined g-C_3N_4 Nanodots in N, S co-doped Hollow Porous Carbon with Boosted Capacity for Lithium-Sulfur Batteries

Han Zhang,[a] Zongbin Zhao,[,a] Ya-Nan Hou,[a] Yongchao Tang,[a] Yanfeng Dong,[b] Shuang Wang,[a]*

Xiaojing Hu,[a] Zhichao Zhang,[c]Xuzhen Wang[a,c] and Jieshan Qiu[,a]*

[a] State Key Lab of Fine Chemicals, Liaoning Key Lab for Energy Materials and Chemical Engineering, PSU-DUT Joint Center for Energy Research, School of Chemical Engineering, Dalian University of Technology, Dalian 116024, China.

[b] Dalian National Laboratory for Clean Energy, Dalian Institute of Chemical Physics, Chinese Academy of Sciences, 457 Zhongshan Road, Dalian 116023, China

[c] School of Chemistry, Dalian University of Technology, Dalian 116024, China.

*E-mail addresses : zbzhao@dlut.edu.cn (Z. Zhao), jqiu@dlut.edu.cn (J. Qiu).

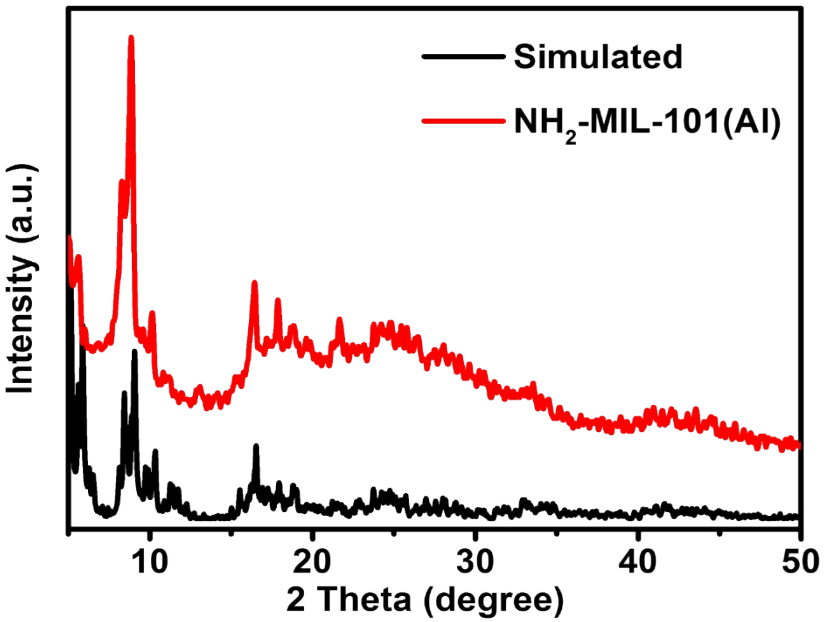

Fig. S1. Powder X-ray diffraction patterns for the simulated NH_2-MIL-101(Al) (black), that obtained from the experiment (red).

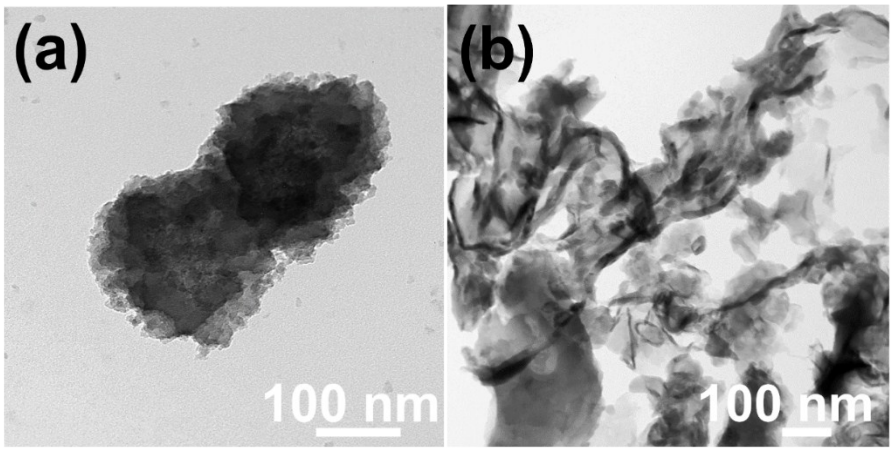

Fig. S2. TEM of images of (a) NH_2-MIL-101(Al), (b) pure g-C_3N_4 obtained through thermal decomposition of ammonium thiocyanate at 600 ^oC for 2h under N_2.

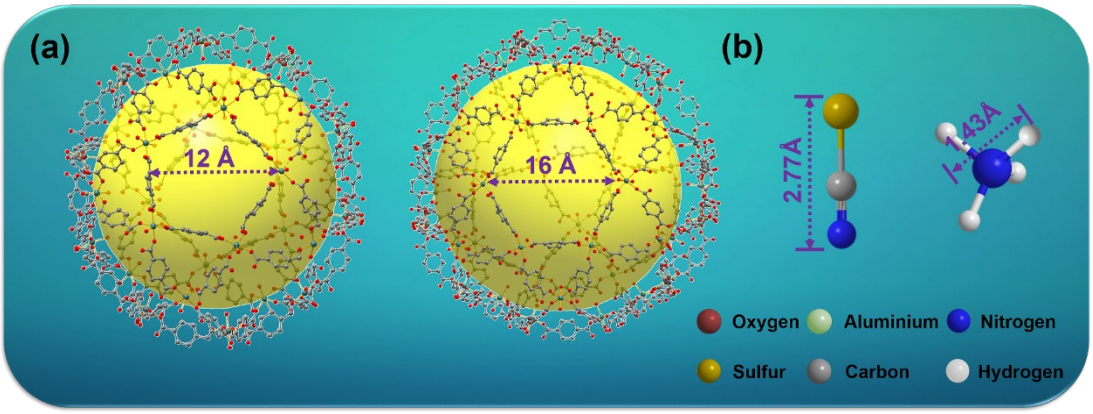

Fig. S3. (a) Detail of the hexagonal and pentagonal window size of NH_2-MIL-101(Al).

(b) ammonium ion and thiocyanate ion size.

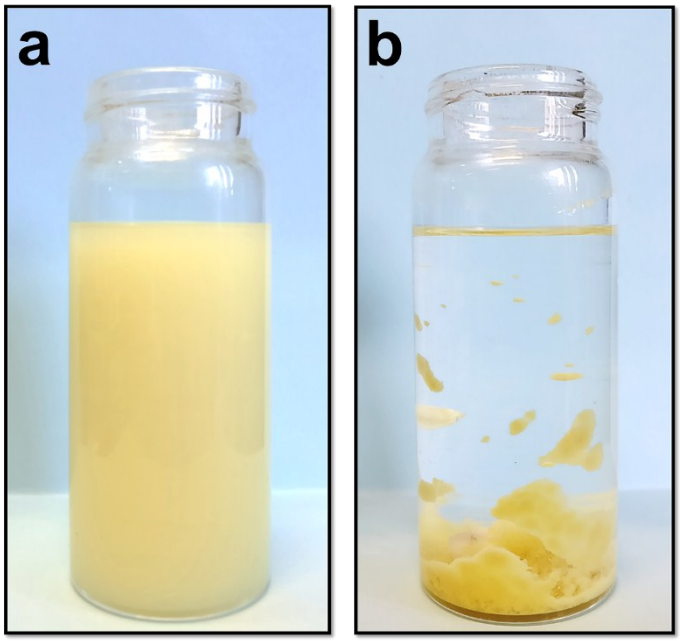

Fig. S4. (a) Before dropwise adding AT solution (NH_2-MIL-101(Al)). (b) After dropwise adding AT solution (AT@NH_2-MIL-101(Al)).

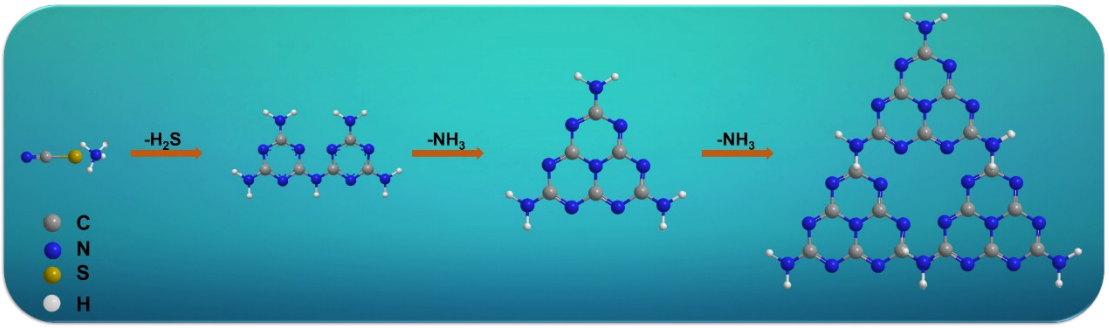

Fig. S5. Schematic illustration of the synthesis of g-C_3N_4 by stepwise polycondensation from ammonium thiocyanate.

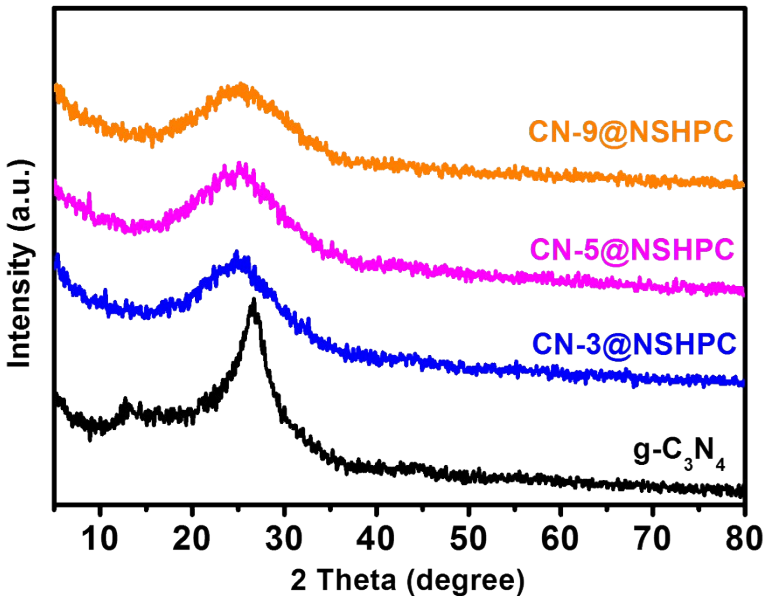

Fig. S6. XRD patterns of g-C_3N_4 and CN@NSHPC. The g-C_3N_4, CN-3@NSHPC, CN-5@NSHPC and CN-9@NSHPC display a diffraction peak at 27°, 25.7°, 26.3° and 26.5°. With the increasing amount of g-C_3N_4, the broad peak between 20° and 30° gradually shifts toward to 27°.

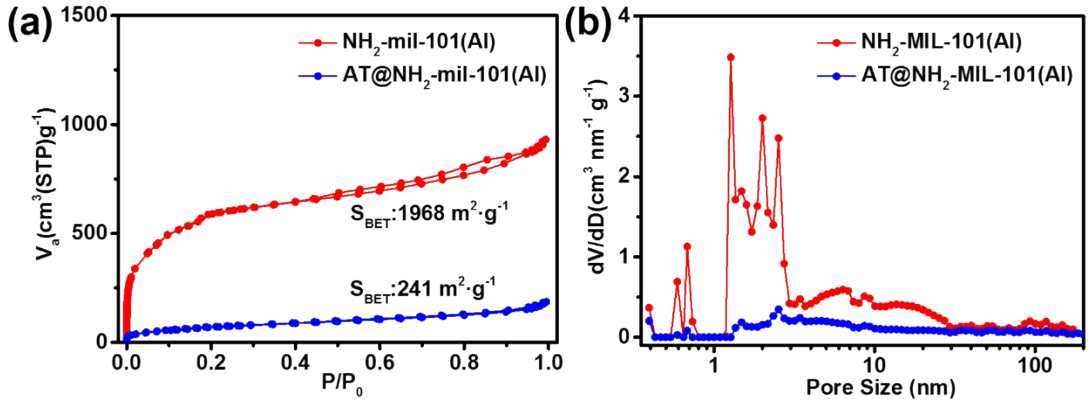

Fig. S7. (a) Nitrogen adsorption isotherms and (b) corresponding pore size distributions of NH_2-MIL-101(Al) and AT@NH_2-MIL-101(Al)

Table S1 Physical characteristics of NH_2-MIL-101(Al), AT@NH_2-MIL-101(Al), g-C_3N_4, NPC, CN-3@NSHPC, CN-5@NSHPC and CN-9@NSHPC.

Sample	BET surface area ($m^2\ g^{-1}$)	Total pore volume ($cm^3\ g^{-1}$)	Average pore diameter (nm)
NH_2-MIL-101(Al)	1968	1.43	2.7
AT@NH_2-MIL-101(Al)	241	0.28	4.4
g-C_3N_4	25	0.16	23.0
NPC	772	1.05	6.1
CN-3@NSHPC	702	0.77	4.4
CN-5@NSHPC	972	1.47	6.0
CN-9@NSHPC	518	0.42	3.2

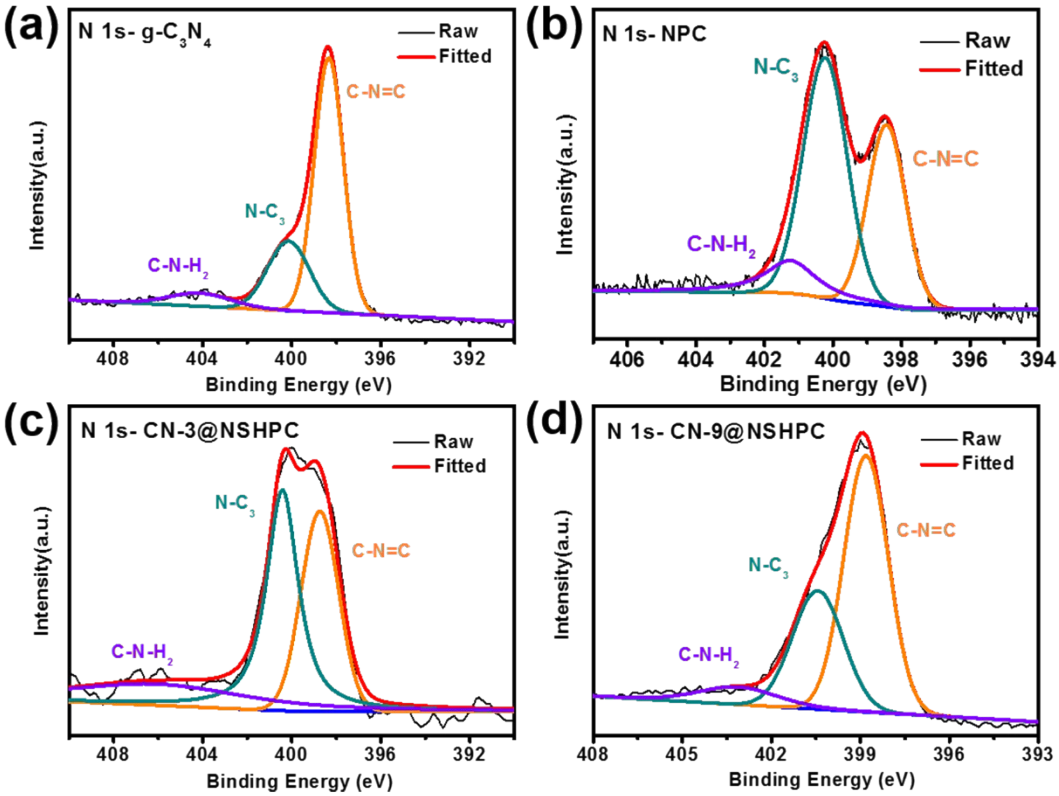

Fig. S8. (a-b) XPS survey spectrum of N 1s (a) g-C_3N_4. (b)NPC (c) CN-3@NSHPC (d) CN-9@NSHPC

Table S2. Summary of nitrogen species and content in CN-3@NSHPC, CN-5@NSHPC, CN-9@NSHPC and g-C_3N_4.

Sample	N content	C-N=C	N-C_3	C-N-H_2
CN-3@NSHPC	10.7	32.9	42.0	24.0
CN-5@NSHPC	13.3	38.9	40.6	20.4
CN-9@NSHPC	37.7	60.1	31.8	8.09
g-C_3N_4	47.2	66.7	25.9	7.37
NPC	8.1	34.5	52.9	12.5

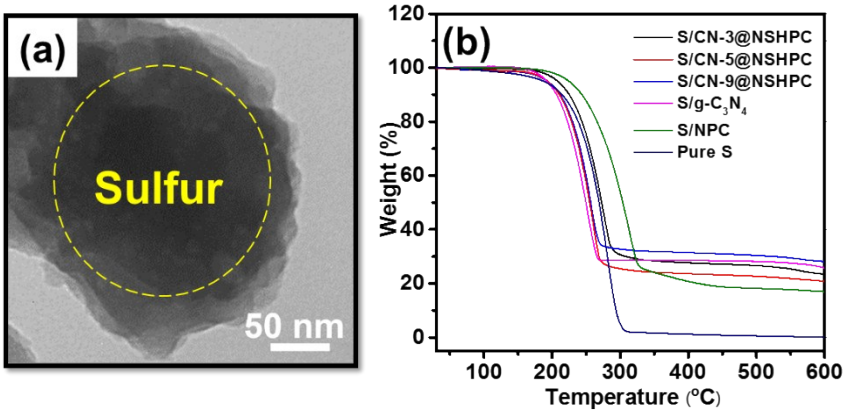

Fig. S9. (a) TEM image of S/CN-5@NSHPC (b) Measurement of sulfur loading on the materials, TGA of S/CN@NSHPC, S/g-C_3N_4, S/NPC and pure S. The result was tested with a heating rate of 10 ^oC min^{-1} at N_2 atmosphere. As shown in the curve of materials, the weight loss of S/CN-3@NSHPC, S/CN-5@NSHPC, S/CN-9@NSHPC, S/g-C_3N_4 and S/NPC are 69%, 73%, 67%, 72% and 73% at 600 ^oC, respectively.

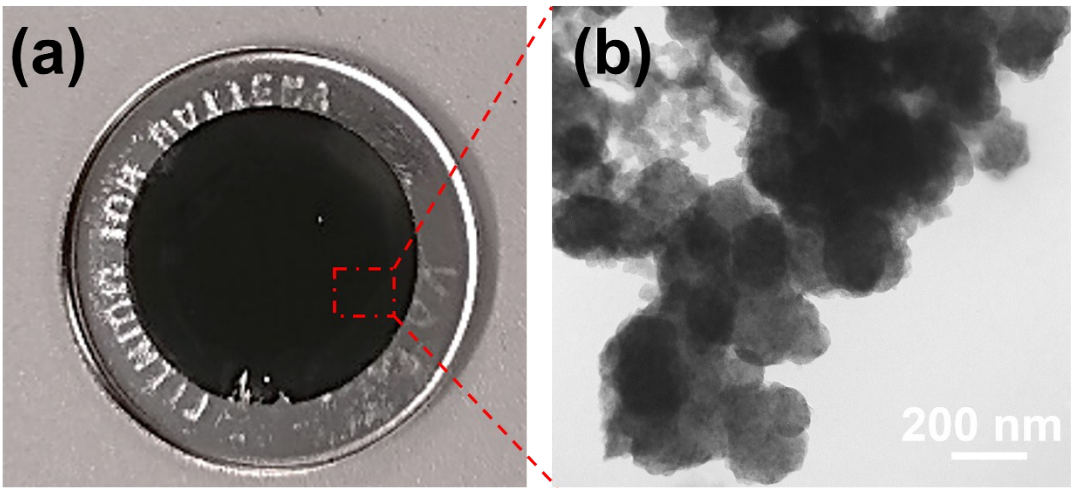

Fig. S10. (a) Digital image of S/CN-5@NSHPC electrode after cycling at 1 C for 500 cycles. (b) TEM image feature the nanostructures of electrode.

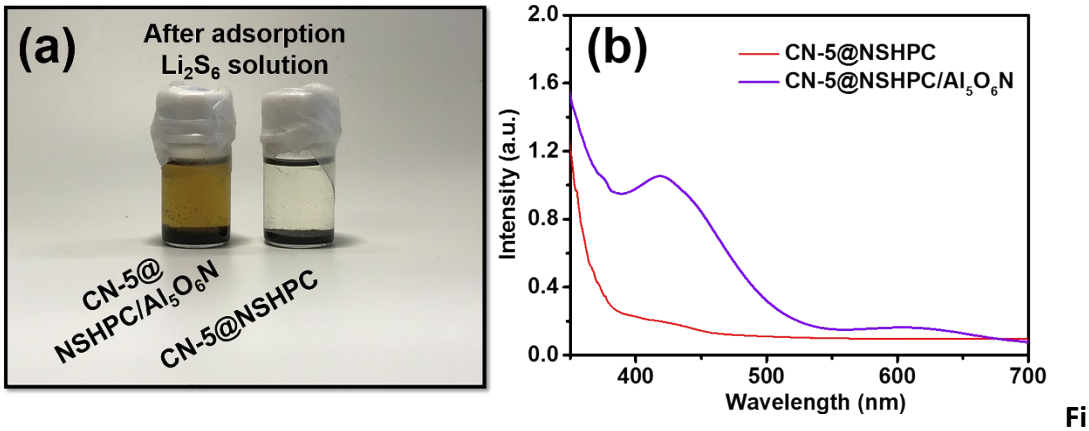

Fig. S11. (a-b) Digital photograph and UV-vis absorption of Li_2S_6 solution before and after the addition of CN-5@NSHPC and CN-5@NSHPC/Al_5O_6N.

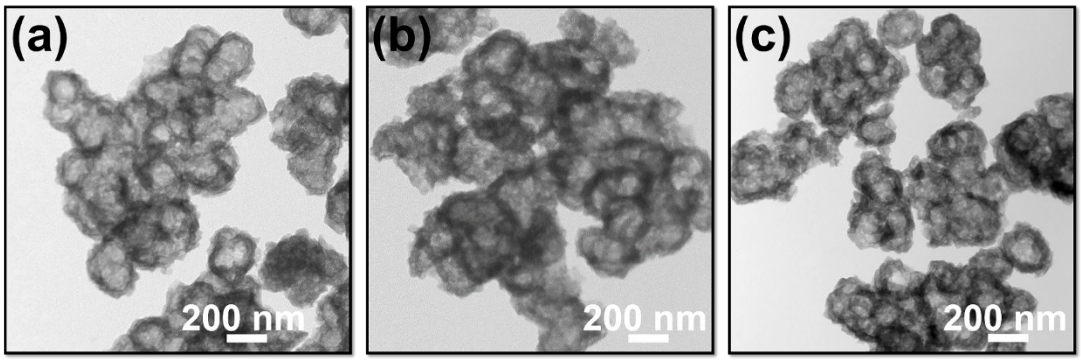

Fig. S12. TEM images of (a) CN-3@NSHPC, (b) CN-5@NSHPC, (c) CN-9@NSHPC.

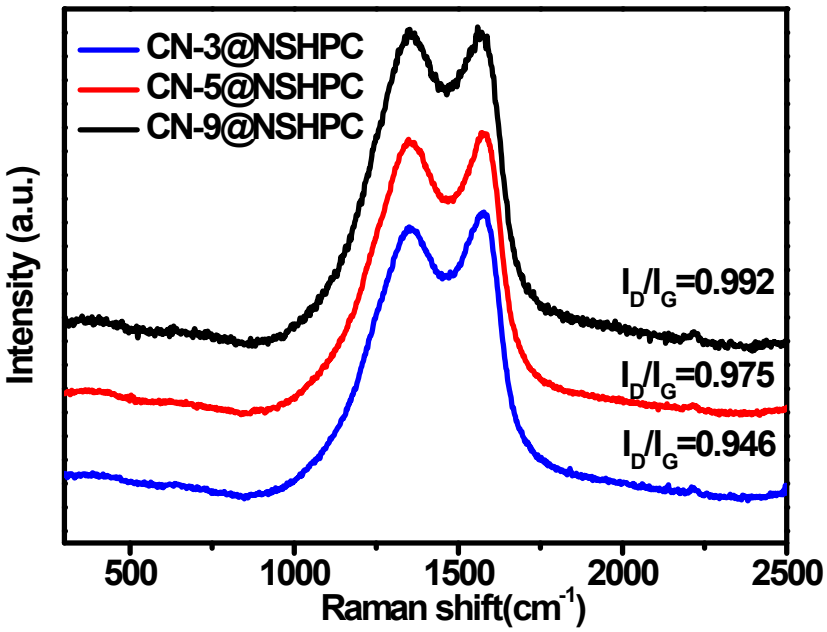

Fig. S13. Raman spectra of CN-3@NSHPC, CN-5@NSHPC and CN-9@NSHPC. The ratio of I_D/I_G rises with the loading amount of AT, especially in CN-9@NSHPC with the highest loading amount of AT. The increasing I_D/I_G indicates that thermal decomposition of AT etches the carbon and results in the formation of more defect sites in the carbon

Table S3 Quantitative elemental analysis of the g-C_3N_4, NPC and CN-x@NSHPC

Sample	I_D/I_G	Elemental Analysis (%)			
		C	H	N	S
g-C_3N_4	-	35.7	1.23	64.2	-
NPC	0.940	72.5	2.7	9.0	-
CN-3@NSHPC	0.946	64.0	3.1	13.5	1.3
CN-5@NSHPC	0.975	60.0	2.6	21.3	2.1
CN-9@NSHPC	0.992	57.4	2.9	26.5	2.7

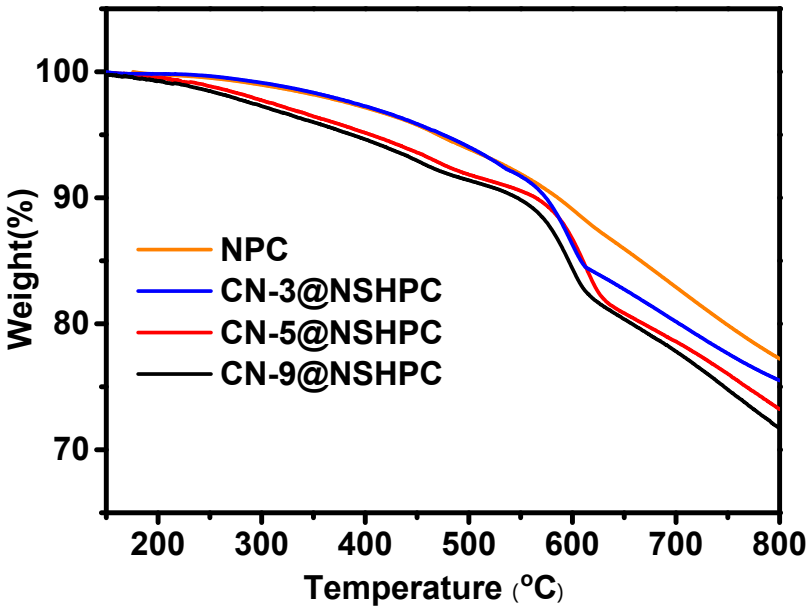

Fig. S14. Comparative thermal gravimetric analysis (TGA) of NPC, CN-3@NSHPC, CN-5@NSHPC and CN-9@NSHPC. The weight loss of CN-3@NSHPC, CN-5@NSHPC and CN-9@NSHPC at 600-650 °C is 1.75%, 4.03% and 6.56%, respectively, corresponding to the decomposition of g-C_3N_4.

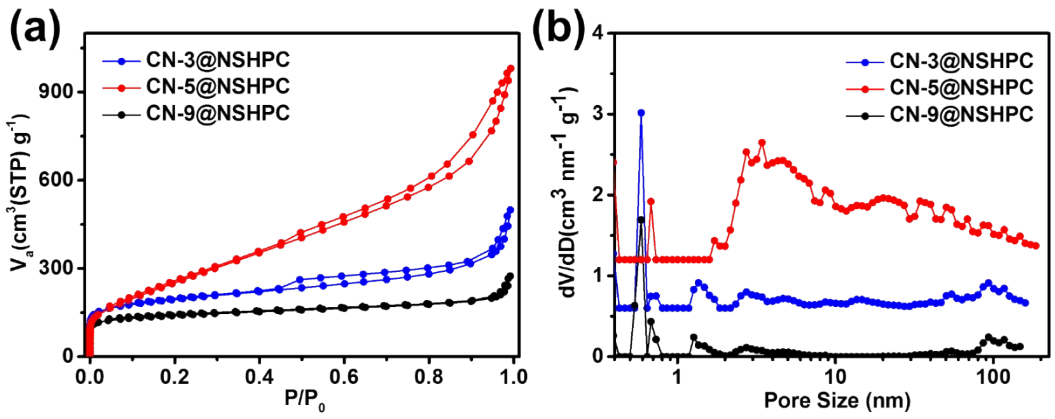

Fig. S15. (a) N_2 sorption isotherms at 77K and (b) pore size distribution of the CN-3@NSHPC, CN-5@NSHPC and CN-9@NSHPC.